

Forced Convection Boiling from a Nonflush Simulated Electronic Chip

J. E. Leland*

Wright Laboratory, Wright-Patterson Air Force Base, Ohio 45433

and

L. C. Chow†

University of Kentucky, Lexington, Kentucky 40506

An experimental investigation has been undertaken to determine the effect of heated surface height on forced convective boiling. An inert fluorocarbon, FC-72 (3M Industrial Chemical Products Division) is circulated through a vertical rectangular channel at velocities of 1–4 m/s and subcoolings of 20 and 35°C. Results for five surface heights, as measured relative to the flow channel wall, were obtained. These were 0.127-mm recessed, 0.229-, 0.457-, and 0.635-mm protruded and flush with the flow channel wall. A reduction in critical heat flux (CHF) occurred at low velocities, while an increase occurred at higher velocities for the protruded cases. A reduction of CHF occurred at all velocities for the recessed condition. Additional results in the velocity range of 5–7 m/s are presented for the flush condition. This data shows that for velocities greater than 4 m/s, CHF becomes weakly dependent on the Weber number. Weak dependence on Weber number also implies a direct proportionality to velocity and a weak dependence on heated length.

Nomenclature

c_p	= specific heat at constant pressure
D_h	= hydraulic diameter
h	= heated surface height
h_{fg}	= latent heat of vaporization
L	= surface heated length
q	= heat flux
q_M	= CHF
q_M^*	= dimensionless critical heat flux
$q_{M,C-C}$	= CHF based on cross-sectional area
$q_{M,Flush}$	= CHF of flush surface
T_f	= fluid inlet temperature
T_{sat}	= saturation temperature
T_w	= heated surface wall temperature
ΔT_{sub}	= subcooling, $T_{sat} - T_f$
V	= bulk velocity, based on channel area
We	= Weber number, $\rho_f V^2 L / \sigma$
ρ_f	= liquid density
ρ_g	= vapor density
σ	= surface tension

Introduction

MUCH work has been done in the area of flow boiling heat transfer using fluorocarbons. The bulk of this work has been directed toward electronic cooling applications and is discussed in the survey paper of Incropera.¹ Substantial studies by Samant and Simon,² Mudawar and Maddox,³ and Mudawwar et al.⁴ have been concerned with heat transfer from simulated electronic chip heat sources that are flush with the flow channel wall. However, Mudawar and Maddox⁵ have studied enhanced surfaces with various fin configurations that protrude into the flow path. McGillis et al.⁶ recently investigated the effect of heated surface protrusion height (0.8–

2.4 mm), for velocities of 9.6–103.9 cm/s and subcoolings of 20–40°C. Heated surface refers to the top surface of the protruding block. They found a reduction in CHF for all combinations of velocity, subcooling, and surface height. CHF is the term given to the point at which a transition from nucleate boiling to film boiling occurs. This transition is marked by a large and rapid temperature excursion that is generally accompanied by burnout of the heating element. Thus, the term “burnout heat flux” is also used to describe this condition.

The thrust of the present work stems from the discovery of Gu et al.⁷ that CHF decreases markedly if the heated surface is not maintained flush with the flow channel wall. This degradation occurred for surface recess and protrusion heights of about 0.1 mm. Because it is difficult to maintain flushness after repeated thermal cycling, even under closely controlled laboratory conditions, it is felt that the same problem may exist under application to electronic chip cooling. Thus, the present effort strives to quantify the effect of nonflush heated surfaces on heat transfer.

Experimental Apparatus

The experimental apparatus has three primary components: 1) the flow loop, 2) flow channel, and 3) heater test section. The flow loop consists of a magnetically coupled centrifugal pump, preheater, flow meters, condenser, and pressure control tank. Figure 1 shows the flow loop system. The preheater is an immersion heater within the flow path and is used to obtain the desired test section inlet fluid temperature. Tap water flowing through the condenser is used to obtain high liquid subcooling and to avoid exceeding the maximum inlet fluid temperature for the pump. Cavitation occurred in the pump if the fluid entering was not subcooled at least 10–15°C. This precluded acquiring data for subcoolings of less than 15°C, except for a few cases.

A pressure control tank allowed independent control of system pressure and was also used for aeration/deaeration of the test fluid. The tank was in communication with the flow path through a vapor line. By regulating the power to a Kapton heater in the bottom of the tank, the pressure at the test section could be controlled.

The flow channel, shown in Fig. 2, had a variable height that remained constant at 6.35 mm for these experiments. An

Presented as Paper 92-0251 at the AIAA 30th Aerospace Sciences Meeting, Reno, NV, Jan. 6–9, 1992; received June 29, 1992; revision received Oct. 6, 1992; accepted for publication Oct. 6, 1992. This paper is declared a work of the U.S. Government and is not subject to copyright protection in the United States.

*Research Engineer, Aerospace Power Division. Member AIAA.

†Professor, Mechanical Engineering Department. Senior Member AIAA.

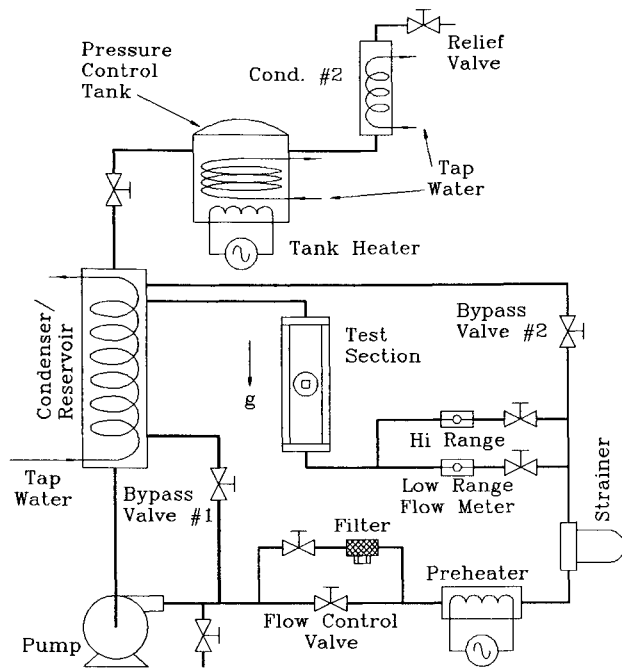


Fig. 1 Flow loop.

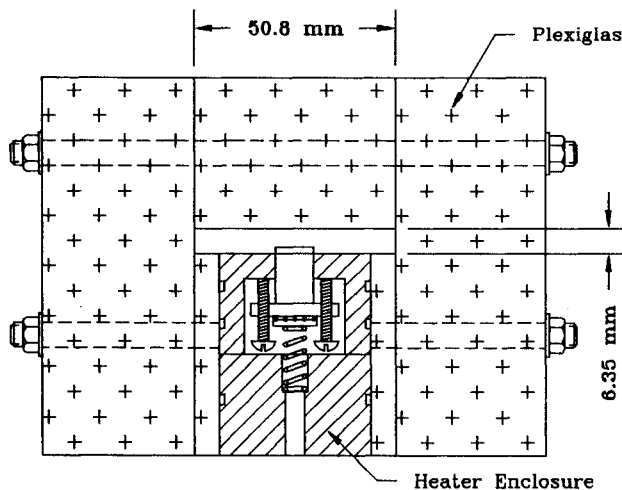


Fig. 2 Flow channel cross section with test heater.

entry length of 137 cm insured fully developed flow for most configurable flow areas. The channel was constructed of optical grade plexiglas for flow visualization purposes. The design allowed both top and side views of the heated surface. Static pressure and fluid temperature were measured at a location 9-cm upstream of the test heater. Because the channel is vertically oriented, a small correction for hydrostatic pressure was made. However, frictional pressure drop and heat loss over this length were assumed to be negligible.

An oxygen-free copper block was used to simulate an electronic device and is shown in Fig. 3. The copper block was enclosed in low thermal conductivity (0.3 W/m-K) Glashterm HT (General Electric Corp.) and heated from the back side by nichrome wire sandwiched between two plates of boron nitride (65 W/m-K). Great care was taken to ensure that the sides of the copper block sealed well against the Glashterm enclosure. High-temperature silicone sealant was used for this purpose. This basic design was proven by Gu et al.⁷ and Mudawar and Maddox.³ Three 0.12-mm wire diameter, type-T thermocouples were imbedded in the block through 0.5-mm-diam holes, and a one-dimensional approximation of heat conduction was made to calculate heat flux. Heat loss, which occurred predominantly through the back of the enclosure, was about 15% throughout the nucleate boiling regime (NBR)

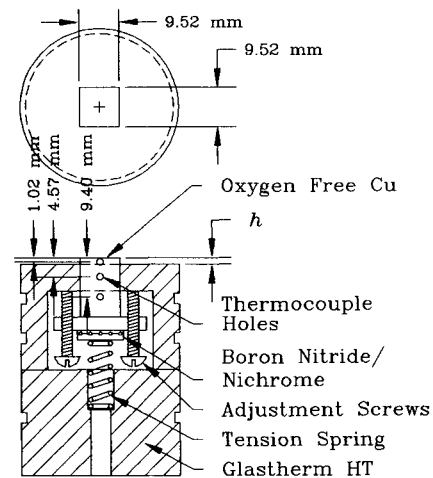


Fig. 3 Copper heater block and enclosure.

up to CHF. Less than 10% heat loss was recorded for a second design used to obtain data for velocities greater than 5 m/s.

The cylindrical design and triple o-ring seal of the heater enclosure allowed quick removal of the test section from the flow channel. A retaining mechanism permitted fine adjustment of the enclosure relative to the channel wall. The retainer also insured that the leading edge remained perpendicular to the flow direction.

Experimental Procedure

Before installation into the enclosure, the exposed face of the copper block was sanded in alternate directions with 1000 grit Wetordry (3M Corp.). Measurements with a surface profilometer confirmed that surface roughness was uniform over the entire face. After installation of the copper block, the height was measured with a micrometer. The surface was then cleaned with methanol to remove finger oil and other residue. The copper block and enclosure were installed into the flow channel and the sealant was allowed to dry overnight before the system was filled with FC-72. Before each day of testing, the fluid was passed through a 7- μ m filter for at least 30 min. The filter was then bypassed and the desired flow rate was attained. The saturation temperature near the test heater was determined from pressure measurement. Power to the preheater and coolant flow rate of the condenser were then adjusted to obtain the desired subcooling.

FC-72 can absorb large amounts of air relative to other common fluids. A typical value at room temperature is 40% by volume. Previous flow boiling experiments by the authors have shown that the effect of absorbed air is negligible over an absorbed air variation of 10–50% by volume. These values were measured using an aereometer (Seaton Wilson, Inc.) connected directly to the flow system. You et al.⁸ have, however, shown that increased air content reduces wall superheat by up to 10°C for pool boiling under decreasing heat flux conditions. This reduction in wall superheat is attributed to the increase in subcooling caused by a reduction of the partial pressure of the FC-72 and increased convection caused by gas bubbles leaving the wall. This latter contribution is probably negligible under flow boiling conditions. In pool boiling experiments using water, Pike et al.⁹ found the effect of absorbed air to die out at higher heat fluxes near the CHF. Forced convective boiling experiments of McAdams et al.¹⁰ exhibited the same behavior. Because deaeration is time-consuming and subsequently requires control of the system pressure (since the system must remain closed to the atmosphere), control of absorbed air was not attempted for the present experiments. The system was operated with the relief valve open to the atmosphere, and air content was about 32 and 45% for the 20 and 35°C subcooling cases, respectively.

Once test conditions were reached, power to the test heater was increased in small increments from single-phase convec-

tion through the nucleate boiling regime to CHF. CHF was determined by increasing power in small increments (<0.5 W) near the point of anticipated CHF until steady state could no longer be achieved and wall temperature rose sharply. The last steady-state value of heat flux was then taken as CHF. Once CHF occurred, the power was quickly shut off and the surface temperature of the copper block typically did not exceed 140°C. Several runs were generally required after a surface had been sanded before repeatable results were obtained. This is a common phenomenon in boiling and is attributed to the establishment of preferred nucleation sites, the release of contaminants and changes in surface microstructure sometimes caused by oxidation.

Uncertainty Analysis

Two test sections were used during these experiments. Test section number one, described above, was used to get all data except that for velocities greater than 4 m/s and a flush heater surface. Test section number two was similar except for a flow channel width of 27.0 mm as opposed to 50.8 mm for test section one.

For all tests, CHF was calculated from the one-dimensional heat conduction equation. For test section number one (Fig. 3), the individual temperatures given by two type-T thermocouples, 4.57 and 9.40 mm from the top surface, were used for this calculation. These were well below the 0.635-mm maximum protrusion height, and thus, gradients produced by heat transfer from the sides of the block should have little effect on accuracy. T_w is extrapolated from the same two thermocouples, and is therefore, an average value. A third thermocouple, 1.02 mm from the top surface, was generally within 2°C of the extrapolated value at this location, and thus was not used in the calculation of T_w in order to maintain consistency with test section two which did not include a third thermocouple. It is realized that radial gradients do exist, especially for the protruded cases, but this method was considered best for obtaining a characteristic wall temperature. Previous results³ give a maximum upstream-to-downstream temperature difference of only 2.2°C for the flush-mounted case. Because of this and the added complexity, additional thermocouples to obtain the surface temperature distribution were not used. Because of the high thermal diffusivity of copper and the distances of the thermocouples from the boiling surfaces, the measured temperatures, and thus the calculated heat flux and wall temperature, fluctuated very little under all conditions but an instability condition discussed later. This unsteadiness translates into a heat flux variance of less than 0.5 W/cm². For test section two, the measured temperature difference of two type-K thermocouples was used, thus

The standard Kline and McClintock¹¹ approach to random uncertainty calculation was taken. The uncertainties of the thermocouples, thermocouple locations, and thermal conductivity were considered. However, the contribution of thermocouple error is dominant for all cases. Because temperature difference is the only variable during testing, the uncertainty in CHF is a decaying function of temperature difference or heat flux. The uncertainty in CHF was calculated for best and worst case temperature difference uncertainties of 0.5 and 1°C. For a temperature difference uncertainty of 0.5°C, the uncertainties in CHF are 13.4, 7.8, and 6.9% for heat fluxes of 34, 85, and 132 W/cm², respectively. For a 1°C uncertainty, the uncertainties in CHF are 24.5, 11.3, and 8.7% for the same heat fluxes.

The repeatability of CHF values was generally within 5% for heat fluxes greater than 50 W/cm². All data is subsequently presented as the average of all available points for a given test section and at a given velocity, subcooling, and heater height. This was done to maintain clarity in the figures. Finally, the bias error was not estimated, however, the percentage of heat loss measured compares with that previously reported³ for a similar design.

Results

Results were obtained for velocities of 1–4 m/s, and two subcoolings, 20 and 35°C. Five heated surface heights were studied, 0.127-mm below, 0.229-, 0.457-, and 0.635-mm above the flow channel wall and flush with the channel wall. Data for velocities up to 7 m/s, as well as subcoolings outside the range mentioned above, were acquired for the flush condition.

Flush

A series of data was obtained for this case to establish a baseline for the nonflush cases and to validate the present test section by comparison with previously obtained data. The single-phase convection and CHF data of the present study agree to within 10% with that of Gu et al.⁷ for all combinations of velocity and subcooling except for 4 m/s and 35°C subcooling. For this case, Gu et al.⁷ obtained a value of CHF that is 25% greater. The reason for this discrepancy is unknown. Data for velocities beyond 4 m/s was obtained using a test heater and flow channel of identical dimensions, except for the flow channel width. The flow channel width for the latter experiments was 27.0 mm as opposed to 50.8 mm.

Mudawar and Maddox³ obtained similar data for vertical upward flow over a flush surface, and for velocity and subcooling ranges of 0.22–4.1 m/s and 0–44°C, respectively. They developed the following predictive correlation based on a physical model of CHF:

$$q_M^{**} = \frac{q_M/(\rho_g V h_{fg})}{(\rho_f/\rho_g)^{15/23} (L/D_h)^{1/23} [1 + (c_p \Delta T_{sub}/h_{fg})]^{7/23} [1 + C_{sub}(\rho_f/\rho_g)(c_p \Delta T_{sub}/h_{fg})]^{16/23}} \quad (1)$$

yielding a higher accuracy. A Helios I (John Fluke Mfg.) data acquisition system was used for these measurements. This device has a resolution of 0.02°C and rated accuracies of 0.45 and 0.39°C for thermocouple types K and T, respectively.

For both test sections, the thermocouple pairs were compared to a precision thermistor (0.1°C accuracy) over the temperature range of the experiments. In both instances, the thermocouples of each pair agreed to within 0.3°C. All the thermocouples agreed with the precision thermistor to within 0.5°C. Thus, the thermocouple accuracies are considered to be well within 1°C for these experiments. The uncertainty of the pressure measurement was 5 Pa. The uncertainty of the flow rate measurement was dominated by the uncertainty of the flow meter which was 0.5% of the reading. Flow velocity was based on channel cross-sectional area. The error in flow velocity due to protruding the surface is less than 2% for the worst case.

or

$$q_M^{**} = 0.161 We^{-8/23} \quad (2)$$

where

$$C_{sub} = 0.021 \quad (3)$$

and the Weber number is defined as:

$$We = (\rho_f V^2 L / \sigma) \quad (4)$$

Equation (1) was reported to be accurate for $We < 10^4$. At near atmospheric pressure, this corresponds to a velocity of about 2 m/s. The present data are plotted against Eq. (2) in Fig. 4. Equation (1) does not collapse the data with respect

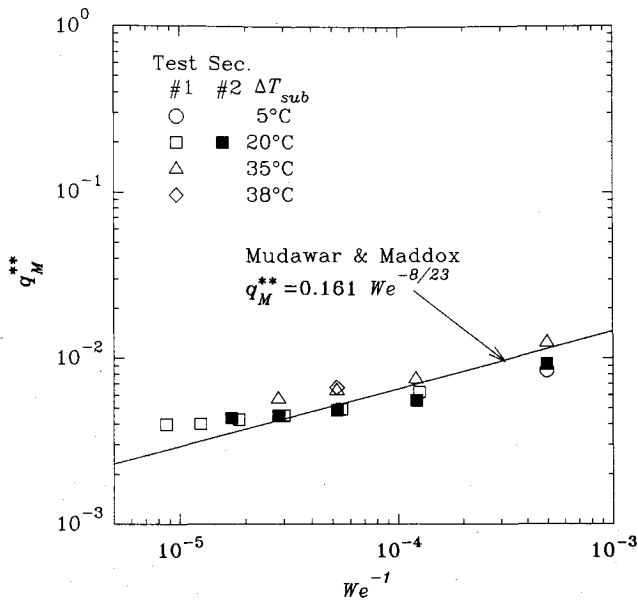


Fig. 4 Comparison of experimental data with Eq. (2).

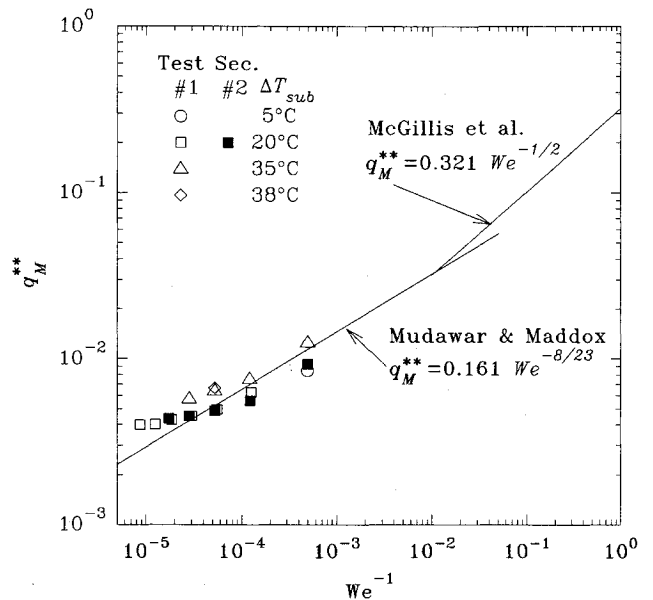


Fig. 5 Comparison of data with Eqs. (2) and (5).

to subcooling, as well as for the data of Mudawar and Maddox.³ The dependence on velocity is in good agreement, however. Data for subcoolings outside of the 20–35°C range suggest that the trend in subcooling is also consistent. This data is also representative of the horizontal orientation for velocities of 3 m/s or greater (i.e., $We^{-1} < 5 \times 10^{-5}$). Previous tests by the authors have shown that even at 45-deg downward flow, the effect was to reduce CHF by only 15 and 5% for flow rates of 1 and 2 m/s, respectively.

Equation (1) shows that CHF is proportional to $V^{7/23}$. Figure 4 shows that as We decreases (i.e., velocity increases), q_M^{**} exhibits a weaker dependence on We^{-1} . Thus, q_M is proportional to V at higher velocities. Furthermore, Eqs. (1) and (2) also imply a weaker dependence on surface tension and more importantly, L . At velocities of 1–2 m/s CHF occurs when the liquid sublayer below the bubble vapor blanket dries out. Since the vapor blanket grows in thickness with the direction of flow, the liquid supply to the most downstream portion of the heater is the most impeded. Thus, dry-out initially occurs at the most downstream portion of the heater. The onset of dry-out was seen to occur almost uniformly over the entire width of the heater. For this mechanism, it is easy to see that CHF is inversely proportional to L .

At higher velocities, the vapor blanket is much thinner and more uniform in thickness over the length of the heater. Mudawar and Maddox³ described the existence of vapor blankets prior to CHF that were much smaller in size than the heated surface area. The liquid sublayer beneath these blankets was fed by liquid from between the blankets instead of from the leading edge of the heater. Because the sublayer is more uniformly fed over the length of the heater, the dependence on L is not as strong as for the low velocity mechanism.

McGillis et al.⁶ conducted similar experiments over the velocity and subcooling ranges of 9.6–103.9 cm/s and 20–40°C, respectively. A lower bound of $We > 100$ was suggested for Eq. (1) as a result of their work. They also suggested the following modification to Eq. (2) for $We < 20$:

$$q_M^{**} = 0.321 We^{-1/2} \quad (5)$$

Figure 4 is expanded to include the correlation of McGillis et al.⁶ in Fig. 5. It is interesting to note the overall trend of q_M^{**} with We^{-1} .

Boiling incipience is generally marked by a sudden and sometimes large temperature excursion (20°C has been reported for some pool boiling tests where FC-72 was used). The thermal shock caused by this excursion is of concern to

those considering direct immersion cooling for electronics. Boiling incipience is stochastic by nature and unavoidable for a given surface and fluid combination. For the present experiments, the boiling incipience temperature overshoot did not exceed 3°C. This maximum occurred at a velocity of 1 m/s and subcooling of 20°C. Temperature overshoot was negligible for most tests and was less than 1°C for all tests where the bulk velocity was greater than 3 m/s.

Incipience generally occurred at a downstream location that was greater than $\frac{1}{3}L$ ($L = 9.5$ mm), as measured from the leading edge. The breadth of the nucleation pattern grew rapidly with increasing heat flux, while the front advanced upstream at a slower rate. The surface was fully nucleated at heat fluxes greater than 80% of CHF. As surface roughness was decreased, nucleation was suppressed and heat fluxes greater than 95% of CHF were required to fully populate the test surface. These results are similar to those previously reported³ and are reported here for later comparison with nonflush data. Departure bubble diameters were estimated to be 0.5 to almost 1 mm for $\Delta T_{sub} = 20^\circ\text{C}$ or less. At higher subcoolings the departure diameters were noticeably smaller.

Recessed Surface

By recessing the heated surface, a shallow cavity in the flow channel wall was created. Flow recirculation zones were consequently established on top of the heated surface at the leading and trailing edges during testing. The thermal boundary layer is thicker in these regions and nucleation should therefore occur first in, or near, these zones. This was true for a flow velocity of 4 m/s where incipience occurred at the leading edge followed by nucleation at the rear edge. For the other velocities, incipience occurred at preferred sites similar to the flush case. A boiling incipience temperature overshoot of 6°C occurred only once and at a velocity of 1 m/s and subcooling of 20°C.

The spread of nucleation sites first in the wake of a preferred site, and then upstream was similar to what occurred for the flush case. The 4 m/s condition was the exception. Following the leading- and trailing-edge nucleation described, preferred sites once again nucleated on the latter $\frac{1}{3}$ of the heated surface. The bubble layer then grew in a manner similar to the lower velocity cases, with the leading-edge bubble layer growing at a much slower rate. The two fronts met in a sudden nucleation of the remaining sites. Throughout this process, nucleate boiling occurred at higher wall superheats, owing to the less effective vapor removal.

A reduction in CHF of 3% over the flush condition was found for a flow velocity of 1 m/s. This reduction increased to 19% for a flow velocity of 4 m/s. Figures 6 and 7 illustrate these reductions more clearly for the two subcoolings explored. For all combinations of velocity and subcooling, except 1 m/s and 20°C, the surface recession results in an 18–30% reduction in CHF.

The above combination should have the lowest reduction for the following reasons. For the flush surface, the ratio of single-phase heat flux to CHF is greatest at this velocity and subcooling. The data show that the single-phase heat transfer coefficient is unchanged by the change in surface height (see Fig. 9). Thus, a decrease in boiling heat transfer would have the least impact. Even so, it must be noted that this case exhibits a disproportionately small reduction in CHF. This anomaly is also displayed (see Fig. 6) by the protruding surface data and only for a subcooling of 20°C. The data for 1 m/s at 35°C subcooling does follow the suggested trend (see Fig. 7). Why this occurs at only one subcooling, and for both recessed and protruded surfaces where different flow patterns and bubble mechanics exist, is unknown. Accuracy is the lowest at low heat fluxes (i.e., low velocities) and a low value of $q_{M,Flush}$ at 1 m/s could explain this anomaly.

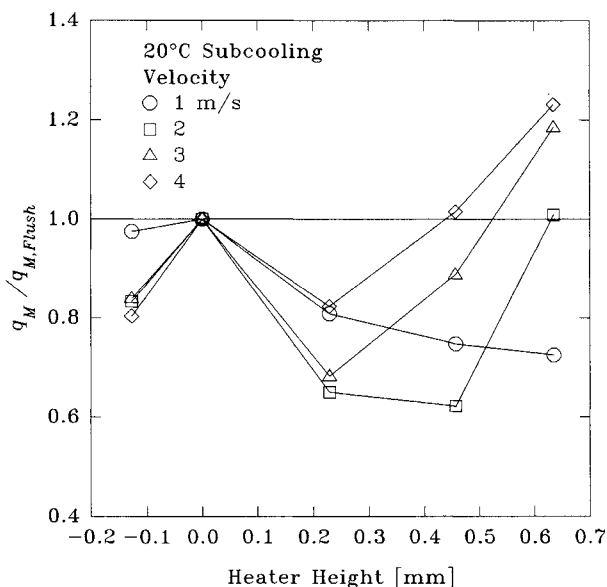


Fig. 6 Variation of CHF with heater height and velocity.

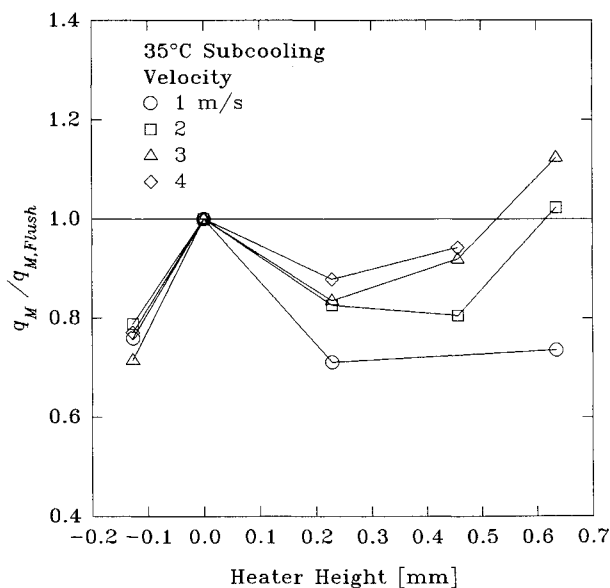


Fig. 7 Variation of CHF with heater height and velocity.

Protruded Surface

The effect on boiling from a surface protruding into the flow stream was studied for h of 0.229, 0.457, and 0.635 mm. For the following results, heat flux is based on an exposed area instead of a cross-sectional area, unless otherwise noted. The exposed area is the total area of the top and sides of the block, while the cross-sectional area is the area of the top only.

For the protruding block, a stagnation point exists at the leading face and separation occurs at the trailing edge. The following describes nucleation as heat flux is increased. First, nucleation occurs on the trailing face while a very small vapor blanket forms quickly after that on the leading face. Nucleation then proceeds from a preferred site on the trailing $\frac{1}{2}$ of the surface while a sheet of vapor, breaking into bubbles, grows from the leading edge (see Fig. 8). However, this sheet of vapor did not grow beyond the leading edge for shorter surface heights and low velocities. Specifically, the vapor blanket did not grow for the conditions $V < 3$ m/s and $h = 0.229$ mm, or $V < 2$ m/s and $h = 0.457$ or 0.635 mm. Bubble generation from these shorter blankets did increase with increasing heat flux. Excluding the above circumstances, the sheet of vapor grew from the leading edge to cover a significant portion of the surface. This was true for 20°C subcooling only. At 35°C subcooling, the vapor sheet grew to a length of only about 1 mm ($L = 9.5$ mm). Nucleation from the sides parallel to the direction of flow was not visible for any case throughout the entire boiling regime.

An interesting instability phenomenon occurred at a flow velocity of 2 m/s and 20°C subcooling for surface heights of 0.457 and 0.635 mm. This instability was marked by the sudden appearance and disappearance of the aforementioned vapor sheet emanating from the leading edge. Remember that the vapor sheet did not exist at 2 m/s for $h = 0.229$ mm. Also, for 35°C subcooling, the vapor sheet never stretched beyond 1 mm, and therefore, remained stable. The alternate pair of panels for 71% of CHF ($h = 0.635$ mm) in Fig. 8 illustrate this event. Near the point of instability, the vapor sheet covered roughly the upstream 50% of the heated surface before breaking into vapor bubbles. The vapor sheet grew steadily up to this point while oscillating with an amplitude of about 1 mm. Just before the instability, the vapor sheet receded to the leading edge and immediately returned to about $\frac{1}{2}L$. The frequency of this occurrence was very unsteady, but was roughly 20 Hz. This large scale oscillation also manifested as an oscillation of T_w .

As power to the heater was further increased, a sudden increase in wall superheat preceded a second stable regime. This temperature excursion is depicted in Fig. 9 by representative data for each heater height case. Note that heat flux is based on the cross-sectional area in Fig. 9, and that $T_w - T_{sat}$ may be obtained by subtracting 20°C from the abscissa. After this temperature excursion, the vapor blanket covered about 60% of the heated surface (see Fig. 8). The vapor sheet length continued to oscillate with an amplitude of roughly 2 mm. As power to the heater was increased, the heat flux increased at almost constant wall temperature. This implies that additional nucleation sites were activated. The 2-mm amplitude oscillation also dies out with increasing power and consequently, surface temperature becomes more steady.

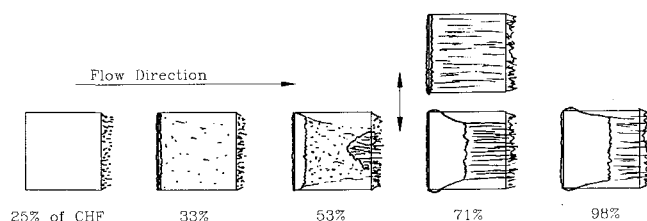


Fig. 8 Procession of boiling and instability for $V = 2$ m/s, $h = 0.635$ mm, and $\Delta T = 20^\circ\text{C}$.

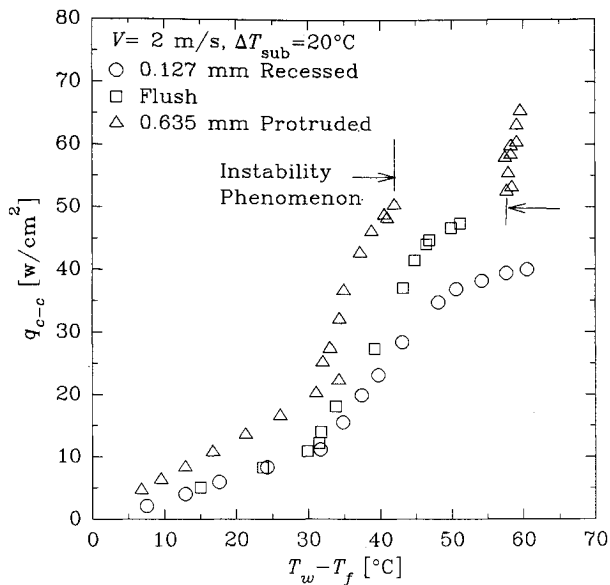


Fig. 9 Behavior of boiling curve with heater height.

CHF occurred more abruptly at lower velocities as compared to the recessed and flush cases. For velocities of 3 and 4 m/s and 20°C subcooling, initial nucleation, bubble-layer and vapor sheet growth occurred as described previously, with the exception of any instability point. The vapor sheet grew to cover about 60% of the heated surface before CHF.

Results for 35°C subcooling are comparable with those for 20°C subcooling, but with the notable absence of any flow instabilities. Comparing Figs. 6 and 7, it can be seen that protrusion height has less of an effect at higher subcooling. This may be due in part to the larger contribution of single phase heat transfer. Unlike water, and to a lesser extent R-12, FC-72 has a low latent to sensible heat ratio, 3.8 and 2.2 for $\Delta T_{\text{sub}} = 20$ and 35°C, respectively. Results for 4 m/s and 35°C subcooling were not obtained due to failure of the nichrome heater wire. However, readings prior to failure indicated an increase of more than 20%.

The behavior of CHF with h is intriguing. Recall Figs. 6 and 7; for a given h , a reduction in CHF occurred for a low flow velocity. As velocity increased, the magnitude of this reduction decreased and an increase in CHF was realized in some instances. For $h = 0.635$ mm, a 20% increase was gained for a flow velocity of 3 m/s. This translated into a 50% increase in power dissipation, which is the real goal of electronics cooling. Power dissipation is simply the product of heat flux and area. If CHF increases with heater height, this product increases at a greater rate, since exposed area also increases. For example, at 20°C subcooling and a flow velocity of 2 m/s, $q_M/q_{M,\text{Flush}} \approx 1$ for $h = 0.635$ mm. Considering the increase in surface area, power dissipation is improved by a factor of 1.27. Figure 10 illustrates how dramatically power dissipation increases with velocity for various h .

Figure 10 also shows that CHF becomes a strong function of V above a certain velocity, 3, 2, and 1 m/s for $h = 0.229$, 0.457, and 0.635 mm, respectively. Because CHF is a stronger function of V for the protruded surface than for the flush surface, there is a point for each h where $q_M/q_{M,\text{Flush}} = 1$. Consequently, an enhancement of boiling heat transfer may be gained for sufficiently large h and/or V . A possible explanation of this increase is that protrusion of the surface creates a favorable flow pattern which has an effect only at higher velocities. The latter two panels of Fig. 8 also illustrate by the narrowing of the vapor blanket that liquid may be feeding from the sides at the downstream portion of the surface. The narrowing of the vapor blanket becomes more pronounced with velocity. Because CHF occurs first at the downstream portion of the top surface, liquid feeding from the sides at this location may be sustaining nucleate boiling.

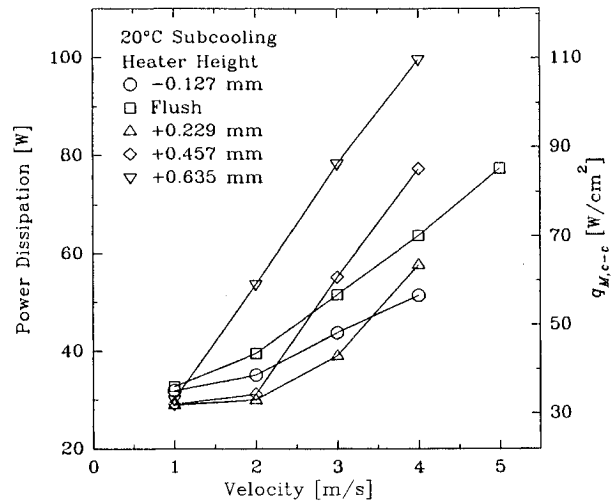


Fig. 10 Variation of maximum power dissipation with velocity and heater height.

The present results, nevertheless, agree with those of Gu et al.⁷ and McGillis et al.,⁶ both of whom found only a reduction in CHF. Gu et al.⁷ obtained results for surface heights within ± 0.1 mm of flush, and a flow velocity and subcooling of 2 m/s and 10°C, respectively. Figure 6 clearly suggests that a reduction is to be expected for these conditions. As mentioned previously, McGillis et al.⁶ obtained results for $h = 0.8$, 1.6, and 2.4 mm over a velocity and subcooling range of 0.10–1.04 m/s and 20–40°C, respectively. Detailed results for $h = 0.8$ and 1.6 mm showed approximately equivalent values of CHF over the entire range of conditions mentioned. These results and those of Fig. 6 imply a decaying rate and possibly limiting value of CHF reduction for increasing h . If this is true, it can be inferred by extrapolation of the data in Figs. 6 and 7 that the present results also agree with those of McGillis et al.⁶ Another indication of agreement is that a 25% reduction in CHF was reported for $h = 0.8$ mm and a velocity and subcooling of 1.04 m/s and 20°C, respectively.⁶ By comparison with the present results, a 27% reduction was found for $h = 0.635$ mm and a velocity and subcooling of 1 m/s and 20°C, respectively. The results of McGillis et al.⁶ and the present investigation suggest that CHF is less a function of h at lower velocities. McGillis et al.⁶ attribute this to a predominant pool boiling mechanism.

The most significant discovery is that for sufficiently large surface height and/or flow velocity, an increase in CHF is obtained. Not only is CHF increased, but power dissipation is increased even more because of increased surface area. This fact should be considered along with CHF by those designing cooling schemes for electronic components.

Conclusions

Flush

1) The dependence of q_M^{**} on We^{-1} becomes weaker as We^{-1} decreases (i.e., velocity increases), especially for $We^{-1} \approx 10^{-5}$. Equation (1) thus implies that q_M is roughly proportional to V at higher velocities (> 2 m/s) as compared to $V^{7/23}$ for lower velocities (≤ 2 m/s).

2) Including the results of McGillis et al.,⁶ Fig. 5 suggests that q_M^{**} is a decaying function of decreasing We^{-1} for We^{-1} less than 1.

3) If Eq. (1) correctly models CHF for $We^{-1} < 10^{-4}$, a weaker dependence of q_M on L is also suggested. This may be explained by a change in the mechanism of liquid supply to the sublayer.

Recessed Surface

1) A reduction of CHF occurred for all combinations of velocity and subcooling. $q_M/q_{M,\text{Flush}}$ gradually decreased with either increased velocity, or increased subcooling.

2) The recessed height of 0.127 mm creates what is considered a very shallow cavity. Further recession of the surface should only yield even smaller values of CHF because the vapor removal mechanism is compromised even more.

Protruded Surface

1) For a given surface height, a decrease in $q_M/q_{M,Flush}$ is experienced at low velocities (<2 m/s for most cases). As velocity increases beyond 2 m/s, $q_M/q_{M,Flush}$ increases to the point where $q_M/q_{M,Flush} = 1$. As heater height increases, the velocity for the condition $q_M/q_{M,Flush} = 1$ decreases.

2) The net increase in CHF at higher velocities may be due to enhanced liquid flow from the sides.

3) Both degradation and enhancement of heat transfer effectiveness are diminished with increased subcooling. This may be explained, in part, by the larger contribution of single-phase heat transfer. The rate of enhancement also diminishes with increasing velocity for both subcoolings.

4) A flow instability phenomenon occurred for heater heights of 0.457 and 0.635 mm. In both cases, the instability occurred at a velocity and subcooling of 2 m/s and 20°C, respectively.

5) A linear dependence of q_M on V is also suggested for protruded height cases by the data of Fig. 10. This dependence occurs at $V > 3$ m/s for a heater height of 0.229 mm and at lesser velocities for the larger heights.

6) A significant increase in total power dissipated is gained by increasing heater height (see Fig. 10). This is because of the combined contributions of increased q_M and greater exposed surface area. For a heater height of 0.635 mm and subcooling of 20°C, a 60% increase in power dissipated (i.e., $q_{M,c-c}$) occurred for velocities greater than 2 m/s.

7) If manufacturing complexity is considered, the enhancement of CHF for velocities of 3 and 4 m/s compares well to the enhancement obtained by Mudawar and Maddox⁵ with the use of structured surfaces.

Acknowledgments

This effort was supported by the University of Kentucky through internal funding. The authors wish to thank the 3M company for their donation of FC-72.

References

- ¹Incropera, F. P., "Convection Heat Transfer in Electronic Equipment Cooling," *Journal of Heat Transfer*, Vol. 110, No. 4, 1988, pp. 1097–1111.
- ²Samant, K. R., and Simon, T. W., "Heat Transfer from a Small Heated Region to R-113 and FC-72," *Journal of Heat Transfer*, Vol. 111, No. 4, 1989, pp. 1053–1059.
- ³Mudawar, I., and Maddox, D. E., "Critical Heat Flux in Subcooled Flow Boiling of Fluorocarbon Liquid on a Simulated Electronic Chip in a Vertical Rectangular Channel," *International Journal of Heat and Mass Transfer*, Vol. 32, No. 2, 1989, pp. 379–394.
- ⁴Mudawwar, I. A., Incropera, T. A., and Incropera, F. P., "Boiling Heat Transfer and Critical Heat Flux in Liquid Films Falling on Vertically Mounted Surfaces," *International Journal of Heat and Mass Transfer*, Vol. 30, No. 10, 1987, pp. 2083–2095.
- ⁵Mudawar, I., and Maddox, D. E., "Enhancement of Critical Heat Flux From High Power Microelectronic Heat Sources in a Flow Channel," *Heat Transfer in Electronics*, American Society of Mechanical Engineers, HTD-Vol. 111, 1989, pp. 51–58.
- ⁶McGillis, W. R., Carey, V. P., and Strom, B. D., "Geometry Effects on Critical Heat Flux for Subcooled Convective Boiling from an Array of Heated Elements," *Journal of Heat Transfer*, Vol. 113, No. 2, 1991, pp. 463–471.
- ⁷Gu, C. B., Chow, L. C., and Beam, J. E., "Flow Boiling in a Curved Channel," *Heat Transfer in High Energy/High Heat Flux Applications*, American Society of Mechanical Engineers, HTD-Vol. 119, 1989, pp. 25–32.
- ⁸You, S. M., Simon, T. W., and Bar-Cohen, A., "Experiments on Nucleate Boiling Heat Transfer with a Highly-Wetting Dielectric Fluid: Effects of Pressure, Subcooling and Dissolved Gas Content," *Cryogenic and Immersion Cooling of Optics and Electronic Equipment*, American Society of Mechanical Engineers, HTD-Vol. 131, 1990, pp. 45–52.
- ⁹Pike, F. P., Miller, P. D., and Beatty, K. O., Jr., "The Effect of Gas Evolution on Surface Boiling At Wire Coils," *Heat Transfer St. Louis, Chemical Engineering Progress Symposium Series No. 17*, Vol. 51, 1955, pp. 13–19.
- ¹⁰McAdams, W. H., Kennel, W. E., Minden, C. S. L., Carl, R., Picornell, P. M., and Dew, J. E., "Heat Transfer at High Rates to Water with Surface Boiling," *Industrial Engineering Chemistry*, Vol. 41, No. 9, 1949, pp. 1945–1953.
- ¹¹Kline, S. J., and McClintock, F. A., "Describing Uncertainties in Single-Sample Experiments," *Mechanical Engineering*, Jan. 1953, pp. 3–8.